Journal of Physics: Conference Series **3195** (2026) 012012 doi:10.1088/1742-6596/3195/1/012012

Development of an innovative wet coating process of graphite bipolar plates to increase the efficiency of PEM fuel cells by optimized water removal

Thomas Klenk[1], Nicolas Weber[1], Wilhelm Wiebe[1*], Andreas Kötzle[2], Beate Ott[2]

[1] DHBW Mannheim, Coblitzallee 1-9, 68163 Mannheim, Germany
[2] OVE Plasmatec GmbH, Carl-Zeiss-Str.10, 71093 Weil im Schönbuch, Germany

[*]E-Mail: wilhelm.wiebe@dhbw.de

Abstract. Fuel cells convert hydrogen into electrical energy, producing only water as a byproduct and emitting no CO_2. A typical proton exchange membrane (PEM) fuel cell consists of a membrane electrode assembly (MEA) and bipolar plates that incorporate gas flow fields. One of the major challenges in fuel cell operation is the management of liquid water, particularly on the cathode side. Excess water can accumulate in the flow channels, leading to gas transport limitations, reduced cell performance, and ultimately degradation of the catalyst layer due to platinum and carbon corrosion. This study focuses on the development of a wet-coating process for bipolar plates using a hydrophobic polymer matrix with highly conductive fillers. The aim is to increase the water contact angle and thereby enhance water removal while maintaining sufficient electrical conductivity. Improved water management minimizes flooding, allowing for stable fuel cell operation with reduced auxiliary power demand for gas recirculation and humidification systems. In addition, the hydrophobic coating provides a potential benefit in terms of corrosion protection for metallic bipolar plates, contributing to extended fuel cell durability and efficiency.

1. Introduction

The development of an innovative wet-coating process for bipolar plates in PEM fuel cells requires targeted improvements in several key areas: corrosion protection, electrical conductivity, hydrophobicity or contact angle, and long-term operational stability. Recent studies have demonstrated that coating metallic bipolar plates with PTFE (Polytetrafluoroethylene) or PTFE-based composite materials can significantly increase hydrophobicity (contact angles above 100°) and thereby enhance water management within the flow channels [1], [2], [3].

It has also been shown that bipolar plates fabricated from composite materials containing carbon-based fillers (e.g., graphite, carbon nanoparticles) can achieve satisfactory electrical conductivity within polymer matrices, meeting the performance targets set by the U.S. Department of Energy (DOE) [4]. One of the DOE's technical objectives for bipolar plates is to ensure that interfacial contact resistance (ICR) values remain below defined thresholds, particularly for coated steel and composite materials [5], [6], [7].

For instance, Zhao et al. (2025) developed a graphite–PVDF (Polyvinylidene fluoride) composite coating on 316L stainless steel using a hot-roll application process. Their results showed a significantly improved ICR of 8.2 $m\Omega \cdot cm^2$ and a contact angle of approximately 96.5°, thereby meeting the relevant DOE 2025 targets [8], [9]. Other studies have shown that PTFE or Ni–P–PTFE coatings influence metal surface roughness and contact resistance, which in turn affects the overall electrical behavior and efficiency of the fuel cell under real operating conditions [10]. Additionally,

metal nitride coatings on aluminum alloys have demonstrated potential for increasing corrosion resistance and hardness. However, challenges remain regarding coating porosity, adhesion, and production costs [11].

Comprehensive reviews have compared a wide range of coating types, including noble metals, metal compounds (nitrides, carbides), amorphous carbon, PTFE hybrids, and polymer-based systems with conductive additives, focusing on their performance in terms of ICR, corrosion current density, and long-term stability under operational loads [9], [3], [12], [13].

In summary, the literature indicates that a promising pathway lies in the development of coatings that effectively combine high electrical conductivity, excellent corrosion protection, and efficient water removal. In particular, the ratio between coating thickness, filler content, and the processing parameters of the wet-coating method plays a decisive role in meeting both the electrical and hydrophobic requirements for advanced bipolar plate applications.

2. Composition of the coating systems

Three different coating formulations based on the commercial binders OVE08T, OVE10T and OVE95T [14] were investigated. Each formulation was applied in two coating cycles on planar graphite plates using a spray deposition process. The primary objective of the different formulations was to adjust the stability of the coating, the wettability of the final surface and the electrical conductivity of the resulting layers.

The OVE08T -based [14] formulation consisted of 10 g OVE08T as binder, 90 g of a 1 wt.% silver dispersion in deionized water and 0.5 g sodium hexametaphosphate as an additive to enhance dispersion stability. The dispersion contained finely distributed silver particles in aqueous medium, which ensured a homogenous coating process. However, due to the low solid content of only 1 wt.% silver, the resulting coatings showed limited electrical conductivity. The addition of sodium hexametaphosphate was essential, as without this stabilizing agent sedimentation of the silver particles occurred over time, impairing homogeneity.

The OVE10T-based [14] formulation was prepared with 40 g OVE10T and 60 g of the same silver dispersion, see Figure 1. To further increase the electrical conductivity, 2 g of additional silver powder were introduced into the formulation. As in the case of OVE08T, 0.5 g sodium hexametaphosphate was added to maintain suspension stability and to prevent particle agglomeration. This formulation therefore combined both the well-dispersed silver phase from the aqueous dispersion and the high solid content from the metallic powder, aiming at a balance between processability and electrical performance.

The OVE95T based formulation, in contrast, applied a three-component silicone binder (100 g OVE95T) combined with 3 g of nanoscale silver powder. In this system, the use of sodium hexameta-phosphate was not required, since the intrinsic properties of the OVE95T binder provided sufficient stability during processing. The incorporation of nanoscale silver powder enabled a high packing density of conductive particles, resulting in superior electrical performance compared to the dispersion-based formulations.

In summary, the OVE08T and OVE10T systems required stabilization by sodium hexametaphosphate due to the use of an aqueous silver dispersion with low solid content, whereas the OVE95T system demonstrated intrinsic stability. The silver phase was introduced either as a low-concentration aqueous dispersion, as a mixture of dispersion and solid powder, or exclusively as nanoscale powder, reflecting different strategies to balance coating homogeneity and electrical conductivity.

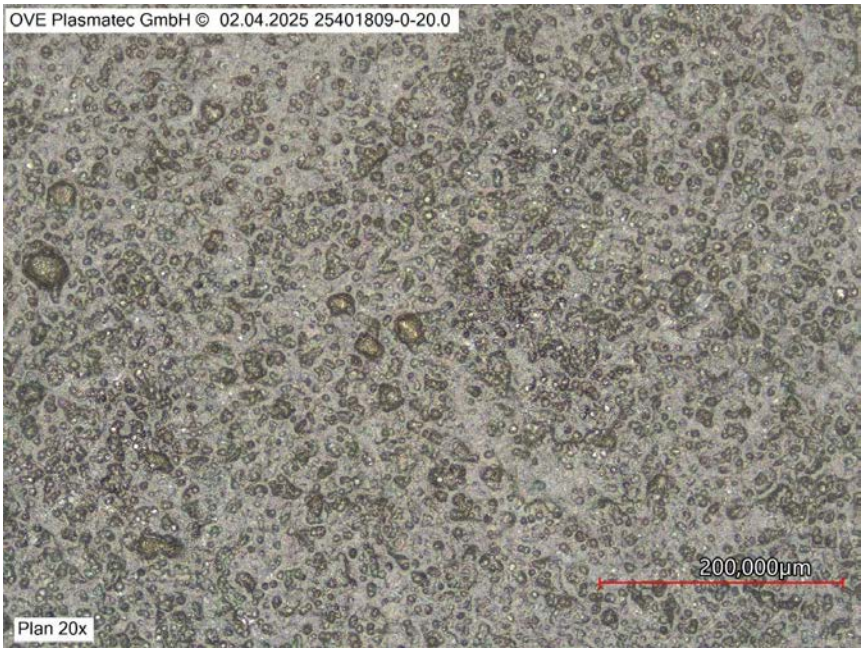

Figure 1. Coating OVE10T [14] with finely distributed silver particles to increase electrical conductivity.

3. Results from the contact angle and electrical resistance measurement

3.1. Static contact angle measurements

The wetting behavior of the coated and uncoated graphite plates was characterized using static and dynamic drop shape analysis with a contact angle measurement system OCA 15EC from DataPhysics Instruments [15], see Figure 2. The setup consists of a liquid dosing system that ensures a reproducible droplet size, a camera with high-resolution optics for recording the droplet shape and determining the contact angle on the coated surface, a magnetic sample table that allows precise positioning of the plate, and background LED lighting to provide uniform illumination of the sample. A close-up image of the measurement setup is shown in Figure 3, in which the four main components of the contact angle measurement system can be identified.

Prior to the actual measurements, a preliminary investigation of the droplet volume was carried out to ensure reproducible drop formation and accurate contact angle determination. Droplet volumes between 2 and 6 µL were tested stepwise using the liquid dosing system. It was observed that at smaller volumes, the droplet occasionally adhered to the syringe tip, preventing proper deposition on the sample surface. Consequently, a fixed droplet volume of 6 µL was selected, as it allowed consistent and reliable application of the liquid onto the coating.

During each measurement, ten water droplets were placed on the surface under identical conditions. The high-resolution camera captured images of all droplets immediately after deposition. Using the evaluation software provided by DataPhysics Instruments, an automatic drop shape analysis was performed to determine the contact angle θ based on the droplet contour. From these ten measurements, an average value was calculated to represent the characteristic contact angle of the respective surface. This procedure was applied for both room temperature and elevated temperature measurements at 80 °C, ensuring comparability between the datasets. This statistical approach minimizes the influence of local surface irregularities and ensures a reliable assessment of the wetting behavior.

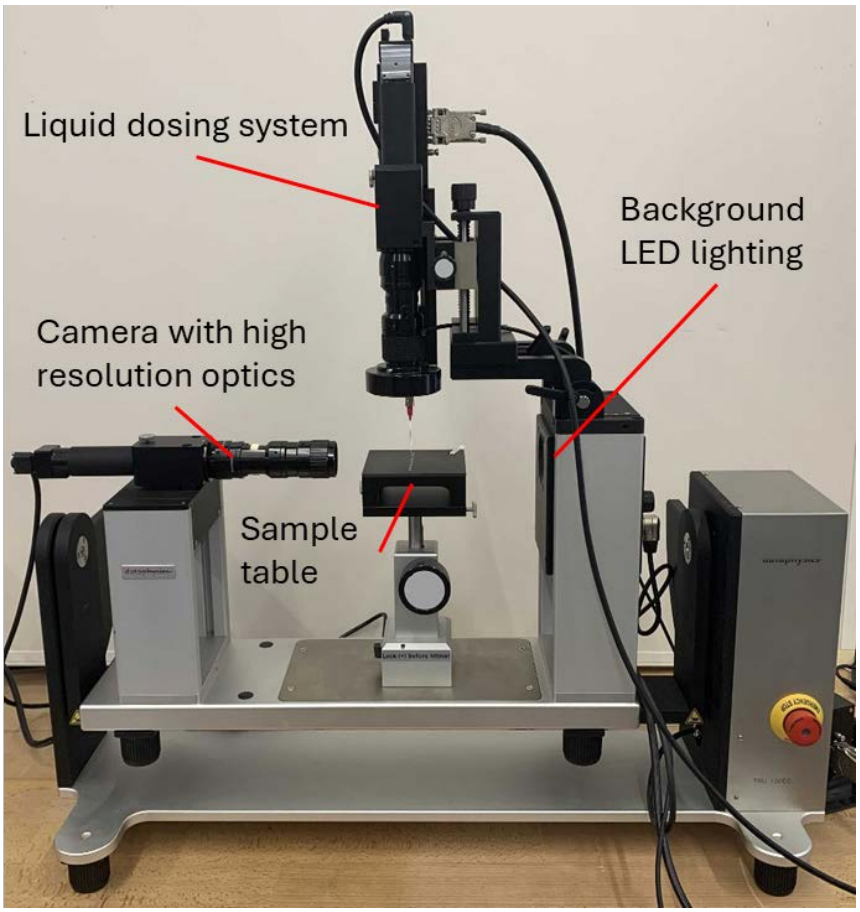

Figure 2. Contact angle measurement system OCA 15EC [15] that was used to determine static and dynamic contact angles.

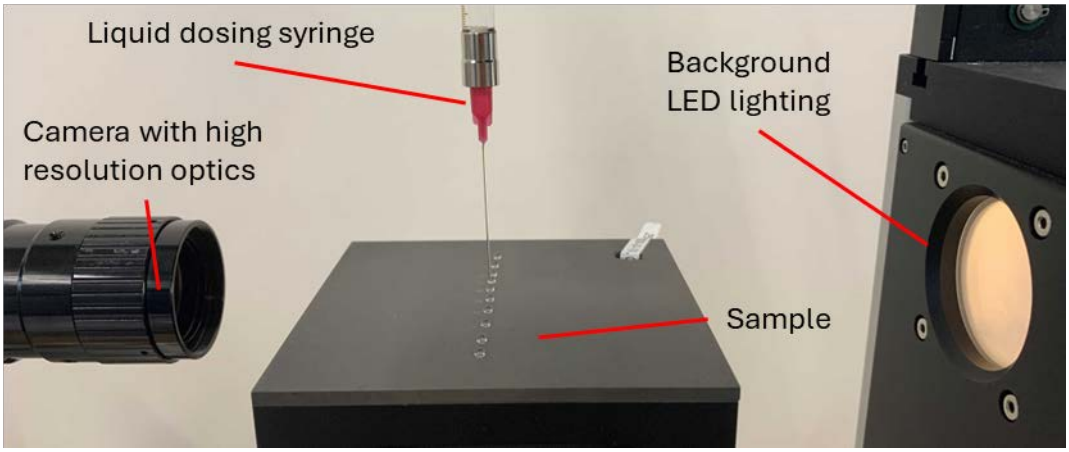

Figure 3. Close-up view of the contact angle measurement setup showing the main components. Ten droplets were placed on each surface, and the average contact angle was calculated to characterize the wetting behavior.

The contact angle θ is defined as the angle formed at the three-phase boundary where liquid, solid, and vapor meet. It provides a direct measure of the interaction between a liquid droplet and a solid surface and is therefore a key parameter for assessing hydrophobicity and surface energy. A high contact angle indicates that the liquid minimizes its interaction with the solid, reflecting a hydrophobic surface, whereas a low angle indicates enhanced wettability.

The static contact angle corresponds to the equilibrium configuration of a droplet placed on a surface. According to Young's equation [15],

$$\cos\theta_Y = \frac{\gamma_{SV} - \gamma_{SL}}{\gamma_{LV}} \quad (1)$$

where θ_Y is the contact angle between the liquid droplet and the solid surface, γ_{SV} the solid-vapor surface energy (surface tension between the solid and the surrounding vapor phase), γ_{SL} the solid-liquid interfacial energy and γ_{LV} the liquid-vapor surface tension. Measurements were conducted at 20 °C and 80 °C to investigate possible temperature effects.

The uncoated reference surface exhibits contact angles around 95° – 97°, indicating moderate hydrophobicity, see Table 1. Application of OVE08T increased the contact angle to ~110°, reflecting a reduction in the solid-liquid interfacial energy. The OVE10T coating showed a slightly lower angle at room temperature (93°), but the contact angle increased significantly at 80 °C (113°), suggesting thermally induced rearrangements of the coating. The silicone based OVE95T yielded the highest static contact angle at 131°, confirming its strong hydrophobic character and suitability for enhancing water management in fuel cell operation. The difference in wettability between the uncoated and OVE95T-coated surfaces is illustrated in Figure 4.

Table 1. Results of the contact angle measurements. The silicone based OVE95T coating with added silver powder shows the highest hydrophobicity compared to the uncoated graphite plate.

Sample	Average Contact Angle (Elliptical Fit) [°]	
	Measurement at 20 °C	Measurement at 80 °C
Uncoated plate, reference	95.2	96.9
2 cycles, 10 g OVE08T, 90 g silver dispersion, 0,5 g sodium hexametaphosphate	110.0	107.1
2 cycles, 40 g OVE10T, 60 g silver dispersion, 2 g silver powder, 0,5 g sodium hexametaphosphate	93.1	112.5
2 cycles, 100 g OVE95T, 3 g silver powder	131.7	131.1

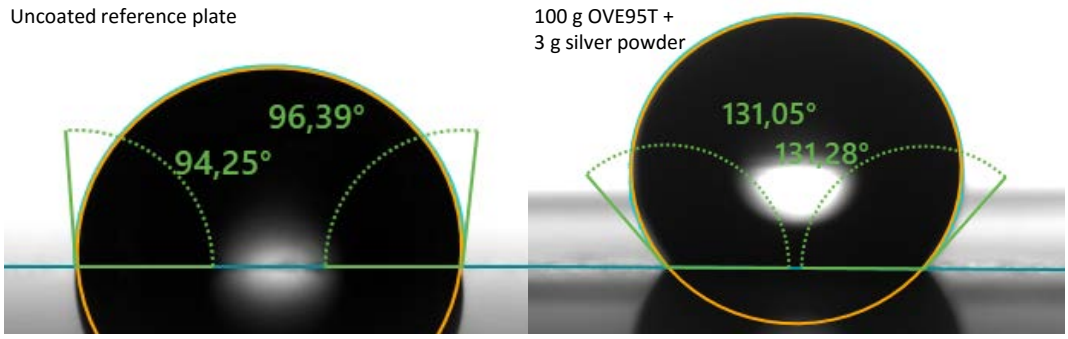

Figure 4. Comparison of static contact angles with 6.5x magnification. Uncoated reference plate (left, ~95°) and OVE95T-coated plate (right, ~131°). The higher contact angle of the coated surface indicates enhanced hydrophobicity.

3.2. Dynamic contact angle measurements

While static contact angles provide insight into surface wettability, they are not sufficient to fully describe droplet mobility on a surface. For this purpose, dynamic contact angle measurements were performed using the tilt stage module of the OCA 15EC. In this method a droplet is placed on the surface and the sample stage is gradually tilted until the droplet begins to move. During this process the advancing contact angle θ_a at the leading edge and the receding contact angle θ_r at the trailing edge

of the droplet are determined. For a schematic representation of the dynamic contact angles refer to Figure 5. The difference between them defines the contact angle hysteresis

$$\Delta\theta = \theta_a - \theta_r. \quad (2)$$

Contact angle hysteresis quantifies the energy barrier that must be overcome for droplet motion. Low hysteresis indicates weak pinning forces and thus easy droplet mobility, whereas high hysteresis reflects stronger retention of droplets on the surface. Complementary to this, the roll-off angle α_s describes the critical tilt angle at which a droplet begins to move. It therefore provides a practical measure of droplet mobility and is closely related to hysteresis and surface roughness.

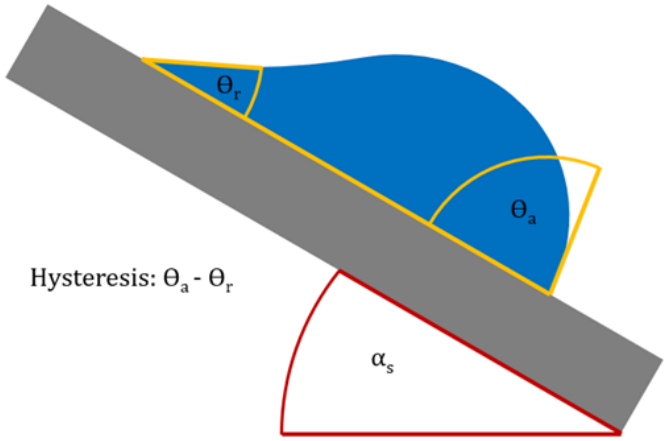

Figure 5. Schematic representation of dynamic contact angle measurement during a tilt stage experiment. The schematic illustrates the principle of dynamic contact angle analysis. When a substrate is gradually tilted, the liquid droplet deforms until the advancing contact angle (θ_a) at the downhill side and the receding contact angle (θ_r) at the uphill side are reached. The difference between these two values defines the contact angle hysteresis. The roll-off angle α_s describes the critical tilt angle at which the droplet starts to move [15].

The uncoated reference plate exhibited a roll-off angle of 63°, in combination with a hysteresis of 71°, see Table 2. These values indicate strong pinning forces and limited water mobility, leading to droplets that adhere strongly to the surface. The OVE10T-coated plate showed a significantly reduced roll-off angle of 43° together with a hysteresis of 56°, demonstrating that droplets detach at lower inclination and water removal is facilitated compared to the uncoated substrate. This behavior is beneficial for minimizing flooding effects in the fuel cell.

Table 2. Results of the tilt-stage experiment performed at 20 °C.

Sample	Tilt-Stage Experiment [°]			
	Roll-off angle α_s	Advancing contact angle θ_a	Receding contact angle θ_r	Hysteresis
Uncoated plate, reference	63.3	87.5	16.5	71.0
2 cycles, 40 g OVE10T, 60 g silver dispersion, 2 g silver powder, 0,5 g sodium hexametaphosphate	43.3	68.1	12.1	56.0
2 cycles, 100 g OVE95T, 3 g silver powder	72.3	139.7	45.0	94.7

[a] The experiment was not carried out with the OVE08T coating, as its adhesion and stability on the surface of the graphite plate were insufficient.

The OVE95T coating displayed a very high advancing contact angle (139°) and a receding angle of 45°, resulting in a larger hysteresis of 94°. The roll-off angle was measured at 72°, which is higher than for OVE10T. Nevertheless, the extremely high advancing angle of OVE95T leads to droplets forming compact, nearly spherical shapes with a reduced contact area to the surface. This geometry, combined with the inherent hydrophobicity of the silicone-based system, favors eventual droplet detachment under operational shear forces, such as gas flow in the fuel cell channels.

Taken together, the results show that while OVE10T offers lower hysteresis and roll-off angles, OVE95T provides the strongest hydrophobic character and droplet compactness, which can be equally advantageous in dynamic operation. Considering both hysteresis and roll-off angle, OVE95T emerges

as a highly promising candidate for water management applications, particularly under conditions where external forces (e.g., gas flow, pressure gradients) support droplet removal.

3.3. Electrical impedance and resistance measurements

In addition to the wetting behavior, the electrical properties of the coated plates are of central importance for their application as bipolar plates in PEM fuel cells. While static and dynamic contact angle measurements provide information on the surface wettability and thus the water management properties of the coatings, the electrical resistance determines the efficiency of electron transfer across the plate. Ideally, a coating should simultaneously exhibit high hydrophobicity to promote effective water removal and a low electrical resistance to minimize ohmic losses. To investigate this aspect, a custom-built resistance measurement setup was designed and employed, as shown in Figure 6.

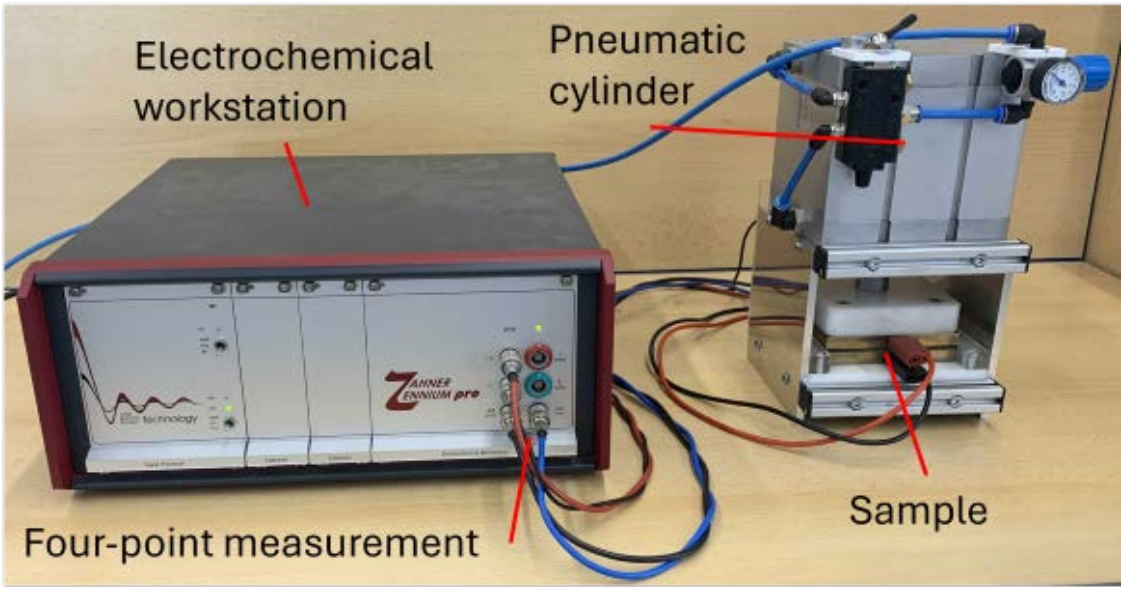

Figure 6. Custom resistance measurement setup for determining the electrical resistance of coated and uncoated bipolar plates. The setup allows simultaneous measurement of impedance and ohmic resistance under controlled pressure conditions, thereby simulating fuel cell operating requirements.

The electrical characterization was carried out using a Zahner ZENNIUM PRO electrochemical workstation, performing both impedance spectroscopy and direct current resistance measurements. A four-point measurement configuration was applied, in which the current-carrying and voltage-sensing leads are separated. This technique effectively eliminates errors caused by contact and lead resistances, allowing for highly accurate resistance determination, particularly in low-resistance systems such as conductive coatings. The measured impedance Z represents the complex opposition of the material to alternating current, combining both resistive and reactive components, whereas the resistance R reflects the purely ohmic part. In fuel cell operation, a low resistance is particularly desirable, as it directly reduces internal voltage drops and thus improves the overall efficiency of the cell. To ensure reproducible mechanical contact conditions during the electrical measurements, a pneumatic compact cylinder ADN-125-50-I-P-A from Festo was integrated into the setup. The applied pressure was set to 1.2 N/cm^2, corresponding to the characteristic clamping pressure in PEM fuel cell assemblies.

The setup incorporates gold-plated copper contact plates with a surface area of 100 cm^2 to ensure a stable and reproducible electrical interface. For a close-up view of the setup refer to Figure 7. The gold plating prevents oxidation of the copper surfaces, which would otherwise lead to the formation of an oxide layer and consequently falsify the measurement results. This design allows for precise determination of both impedance and ohmic resistance under defined mechanical and electrical conditions, ensuring reproducible and comparable data between coated and uncoated samples.

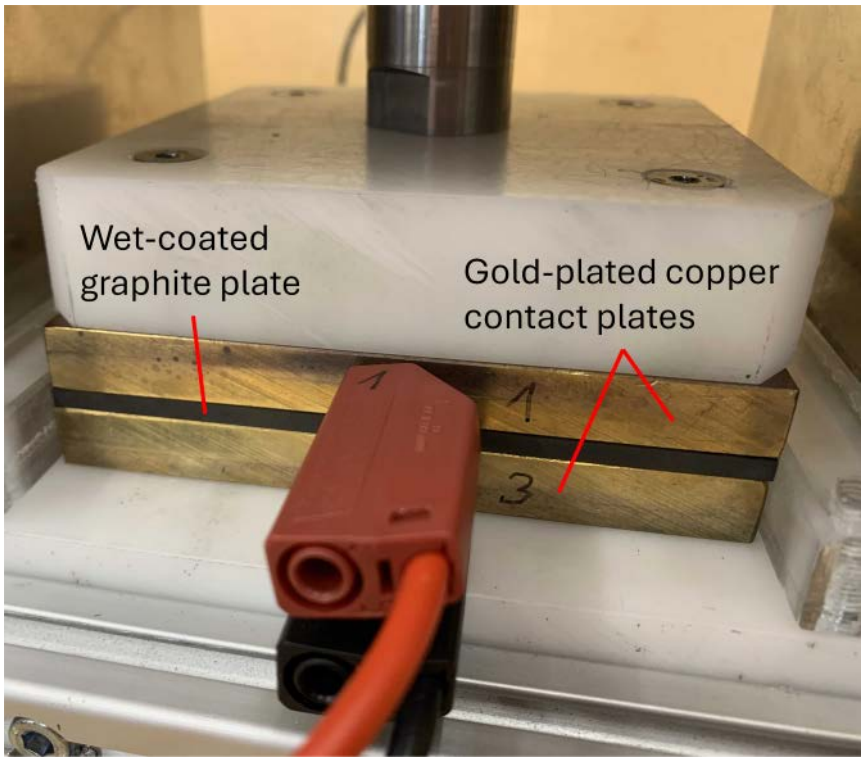

Figure 7. Close up view of the resistance measurement setup. The wet-coated graphite plate is clamped between two gold-plated copper contact plates.

The uncoated reference plate exhibited a very low ohmic resistance (0.023 mΩ), see Table 3, but did not provide any surface modification with respect to wettability. The OVE10T-based system showed a higher resistance of 0.930 mΩ, indicating an increase compared to the reference. This can be attributed to the combination of the aqueous silver dispersion and the additional silver powder. While this improves conductivity compared to purely dispersion-based systems, it still results in higher interfacial resistances. The main reasons are incomplete particle packing and the influence of the binder.

In contrast, the OVE95T-based formulation achieved a markedly improved balance of properties. With an impedance of 5.1 mΩ and an ohmic resistance of 0.633 mΩ, this system provided the lowest resistance among the coated plates. The use of nanoscale silver powder in combination with the silicone-based OVE95T binder enabled a dense and stable conductive network within the coating, reducing electron transport barriers. Importantly, this formulation also demonstrated the most favourable wetting properties, thereby combining effective water management with superior electrical performance.

Table 3. Results of the impedance and resistance measurements. The resistance of the OVE95T coating is slightly higher than that of the uncoated reference plate, but it represents the best performance among the investigated coating systems.

Sample	Impedance Z (mΩ)	Resistance R (mΩ)
Uncoated plate, reference	1.0	0.023
2 cycles, 40 g OVE10T, 60 g silver dispersion, 2 g silver powder, 0,5 g sodium hexametaphosphate	1.3	0.930
2 cycles, 100 g OVE95T, 3 g silver powder	5.1	0.633

[a] The experiment was not carried out with the OVE08T coating, as its adhesion and stability on the surface of the graphite plate were insufficient.

In summary, the OVE95T-based coating system proved to be the most promising candidate, as it successfully unites hydrophobic surface behaviour with a sufficiently low electrical resistance. This dual functionality is essential for fuel cell applications, where both efficient water removal and minimal electrical losses determine long-term stability and performance.

4. Single-cell fuel cell testing

After the detailed material characterization in terms of wettability and electrical resistance, the next step was to evaluate the coated plates under real operating conditions in a PEM fuel cell environment. For this purpose, experiments were carried out using the balticFuelCells quickCONNECTfixture [16] equipped with a low-temperature PEM fuel cell featuring an active area of 50 cm². This setup provides a highly flexible and reproducible testing platform, in which bipolar plates can be exchanged rapidly without compromising sealing or alignment. To ensure precise control of operating parameters such as cell temperature, gas humidity, flow rates, and inlet pressures, the system was connected to a FuelCon fuel cell test station, Evaluator C600 [17], shown in Figure 8. This test station enables the recording of polarization curves and long-term durability tests under well-defined conditions. The system proved to be particularly advantageous for the present study, as it allowed a consistent comparison of different coatings under identical operating conditions.

The electrochemical performance of the coated and uncoated graphite plates was evaluated under defined operating conditions on the FuelCon test bench. The test parameters were chosen to represent realistic PEM fuel cell operation and are summarized in Table 4. During all measurements, both hydrogen and air were fully humidified to ensure stable membrane hydration, while the cell temperature was maintained at 80 °C. A cell voltage of 0.6 V was applied, corresponding to typical operating conditions of PEM fuel cells under load. Gas flow rates and pressures were continuously monitored at both the inlet and outlet to enable a detailed analysis of the cell’s fluidic and electrochemical behavior.

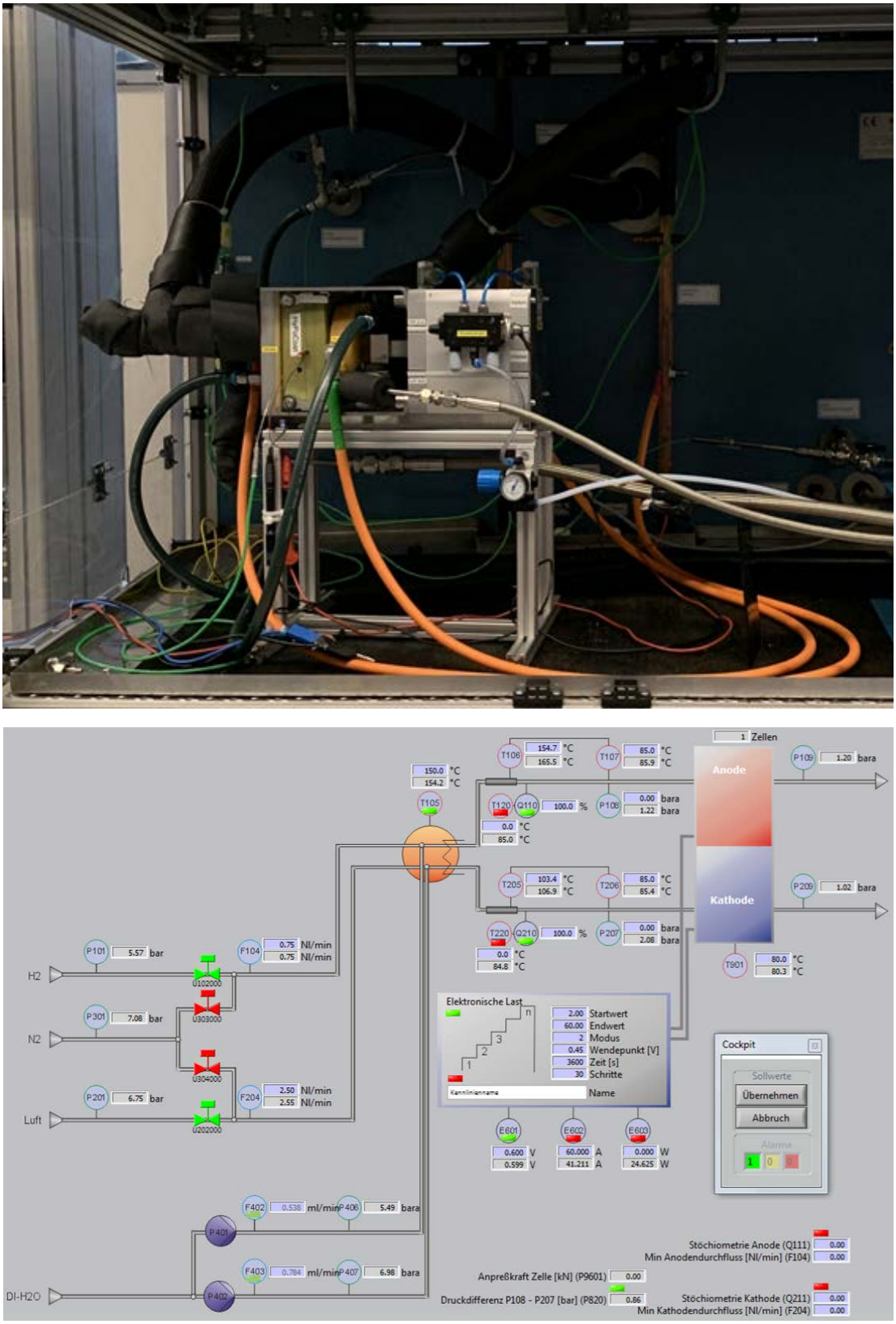

Figure 8. Setup of the EHC in the FuelCon test station [18] (top) and its schematic representation (bottom). The photograph on the top shows the actual test bench used for single-cell characterization of the bipolar plates. The schematic below illustrates the modular structure of the system, including the gas supply, humidification units, heating, and electronic load. The corresponding tag numbers used in the diagram are explained in Table 4.

Table 4. Test conditions and signal tags used for all single-cell measurements on the FuelCon test bench.

Tag number	Description	Test conditions
F104	H_2 flow rate	0.75 NL/min
F204	Air flow rate	2.5 NL/min
T107	H_2 inlet temperature	85 °C
T206	Air inlet temperature	85 °C
Q110	H_2 humidification	100 % relative humidity
Q210	Air humidification	100 % relative humidity
T901	Cell temperature	80 °C
E601	Cell voltage	0.6 V
P108	H_2 inlet pressure	measured
P207	Air inlet pressure	measured
P109	H_2 outlet pressure	measured
P209	Air outlet pressure	measured
E602	Cell current	measured

In the following, two types of bipolar plates were selected for direct comparison, an uncoated reference plate and a plate coated with OVE95T containing silver powder, identified previously as the most promising formulation. The evaluation consisted of several stages. First, U-I polarization curves were recorded to determine the fundamental electrochemical performance. Subsequently, long-term operation tests were conducted by applying a constant cell voltage over several days, while continuously recording the current. In addition, cyclic voltammetry (CV) and electrochemical impedance spectroscopy (EIS) were performed before and after the polarization measurements and long-term stability tests to detect possible changes in electrochemical behavior or interfacial resistance. This procedure enabled an assessment of the coating stability and its influence on sustained fuel cell performance.

4.1. Polarization curves

The polarization curves in Figure 9 compare the performance of an uncoated reference plate with a plate coated using the optimized OVE95T formulation containing silver powder. Measurements were conducted at a cell temperature of 80 °C under fully humidified gas conditions. At low current densities (high cell voltages), the coated plate exhibits slightly higher voltages compared to the uncoated reference, indicating a reduced ohmic and interfacial resistance.

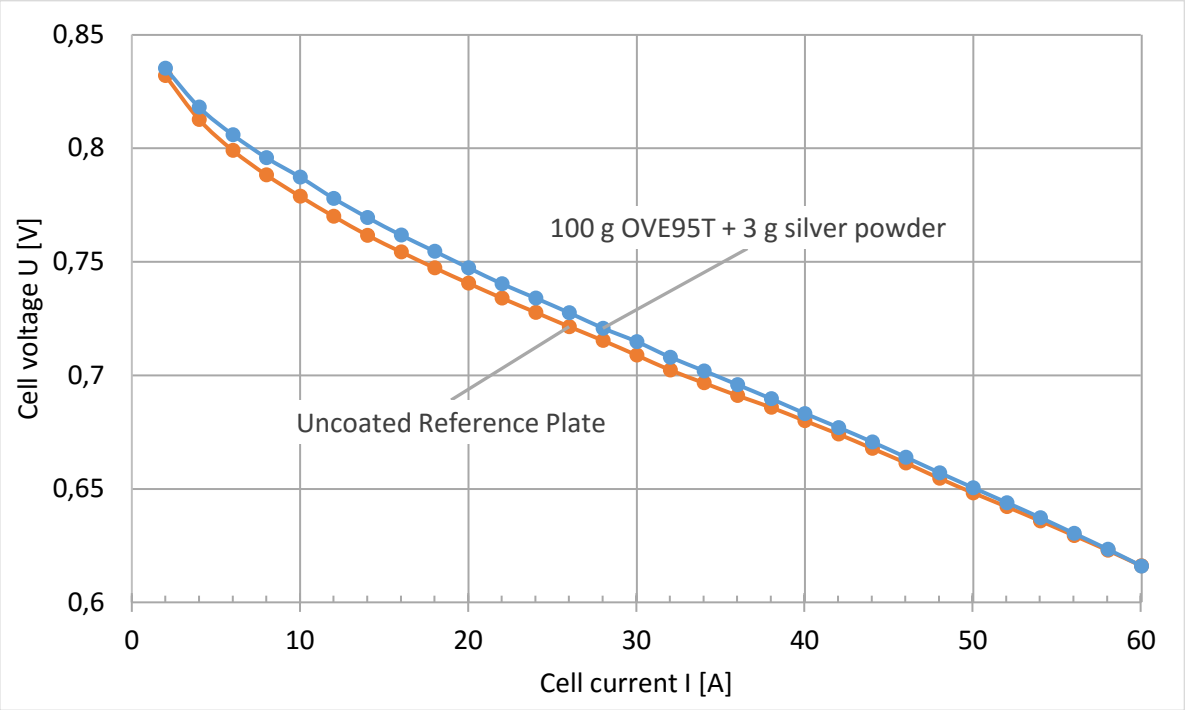

Figure 9. Polarization curves of an uncoated reference bipolar plate and a coated plate with OVE95T and silver powder at 80 °C cell temperature and fully humidified reactant gases. Both curves display the characteristic decrease in cell voltage with increasing current density, reflecting the interplay of activation, ohmic and mass transport losses within the fuel cell.

This improvement is most pronounced in the kinetic region of the polarization curve, where electrode and interfacial processes dominate. With increasing current density, the curves gradually converge, and in the ohmic and mass transport regions the difference becomes less distinct, although the coated plate still maintains a marginal advantage. Importantly, the coated plate maintains a smooth and stable curve progression without abnormal deviations, indicating that the introduction of the hydrophobic OVE95T layer with conductive silver fillers does not disrupt the fundamental electrochemical processes at the electrode–electrolyte interface. Although the coating introduces an additional interfacial layer between the graphite plate and the gas diffusion layer, the electrical conductivity remains sufficiently high to enable effective charge transfer. The silver powder within the OVE95T matrix ensures good electronic pathways, while the hydrophobic silicone-based binder contributes to enhanced water management.

Overall, the results demonstrate that the OVE95T-based coating with silver powder does not introduce additional resistive losses; instead, it even provides a measurable performance improvement in the kinetically controlled regime. This indicates that the coating enhances interfacial contact and supports stable charge and mass transport. These findings are particularly relevant since the coating also improves hydrophobicity and water management, as shown in previous contact angle experiments, thereby combining favorable surface properties with maintained or even slightly improved electrical performance.

4.2. Long-term operation

The long-term stability of the fuel cell system was investigated under constant operating conditions (see Table 4). During the durability test, all data were recorded with a measurement rate of 10 s and subsequently evaluated to monitor cell performance and identify possible degradation effects over time. Figure 10 illustrates the current evolution over a test duration of 144 hours. The uncoated balticFuelCells reference plate shows higher absolute current values compared to the OVE95T-coated plate containing silver powder. As expected, both the uncoated reference plate and the OVE95T-

coated plate show a gradual decline in current density over time, reflecting the typical performance decay in long-term fuel cell operation due to aging phenomena, membrane dehydration, or flooding effects.

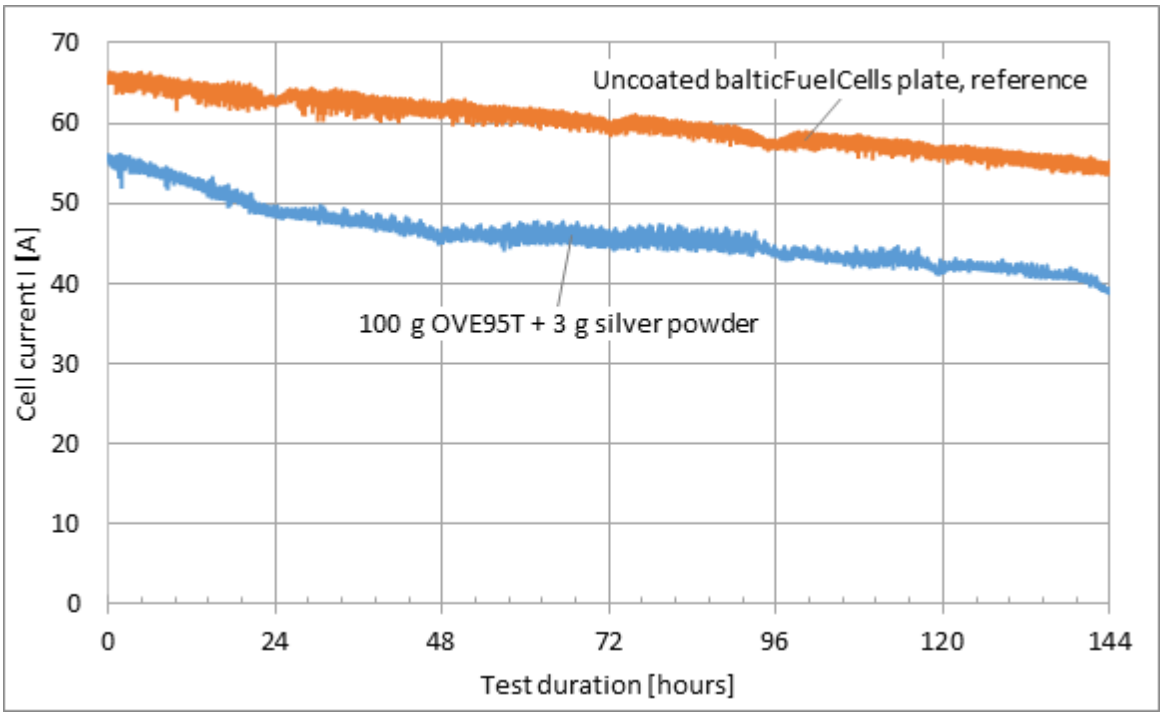

Figure 10. Cell current during long-term operation at constant cell voltage (U = 0.6 V, T = 80 °C, 100 % relative humidity). The diagram shows the current density development of a single cell over a period of 144 hours for two different bipolar plate configurations. The results indicate that the applied coating has an influence on the electrochemical performance of the fuel cell.

The reference plate consistently delivered higher current values throughout the experiment, starting from about 66 A and decreasing to approximately 55 A. In comparison, the coated plate began at around 56 A and stabilized at roughly 40 A by the end of the test. At first glance, this difference suggests lower electrical performance of the coated plate under the given conditions. However, it is important to note that these results should not be interpreted solely as a loss of efficiency. The OVE95T-based coating fundamentally alters the wetting behavior of the bipolar plate, as evidenced by the static and dynamic contact angle measurements. The higher hydrophobicity supports more effective water droplet removal from the flow fields, reducing the risk of local flooding. This effect is particularly relevant under dynamic load changes, where transient water accumulation can cause severe performance fluctuations. Although the polarization curve indicated a slightly higher ohmic resistance for the coated plate, this trade-off can be compensated during long-term operation by more stable water management and potentially reduced degradation rates.

Overall, the current-time data demonstrate that the application of the OVE95T coating results in a stable and reproducible behavior over extended operation. The absence of irregular fluctuations or accelerated degradation is a positive indication of coating stability. These results suggest that the coating is not only chemically durable under fuel cell operating conditions, but also provides functional advantages that may become more pronounced in long-term stack operation, where water management and system-level efficiency are decisive factors. Another critical aspect is the interaction between hydrophobicity and gas flow behavior. The coated surface, by reducing water retention, contributes to a lower pressure build-up on the cathode side, as will be discussed in the following section. This reduces the auxiliary power consumption of the air compressor, which in practical fuel cell systems represents a substantial fraction of the total parasitic load. Hence, while the immediate

cell current is somewhat lower, the net system efficiency may still benefit when the reduced auxiliary energy requirements are taken into account.

4.3. Cathode pressure

In addition to the electrochemical performance, the influence of the coating on the cathode inlet pressure was evaluated, as shown in Figure 11. The uncoated reference plate exhibits a higher and nearly constant inlet pressure of about 2.1 bara, whereas the OVE95T-coated plate with silver powder stabilizes at a lower pressure level of approximately 1.9 bara. Both curves exhibited remarkable stability, without signs of fluctuations or gradual increases, confirming that no flooding or significant flow obstruction occurred in either case.

The consistently reduced pressure level observed with the coated plate, however, is of particular advantage. In fuel cell systems, a substantial fraction of the parasitic power demand originates from the air compressor required to provide oxygen to the cathode. Higher cathode pressures directly translate into greater compression work and, consequently, into a larger share of the gross fuel cell power being consumed by auxiliary components rather than delivered as usable output. By maintaining a lower cathode pressure, the coated plate reduces the load on the compressor, thereby lowering parasitic losses and effectively increasing the net power output of the fuel cell system.

Consequently, although the coated plate shows a somewhat lower absolute electrochemical performance in terms of current density, the reduced cathode pressure can offset this drawback at system level by lowering the auxiliary power demand and thereby enhancing the overall energy efficiency. This result underlines that the coating not only improves water management through enhanced hydrophobicity but also contributes to the energy efficiency of the entire system. By reducing the required cathode backpressure while maintaining stable operation, the developed coating demonstrates a dual benefit. It ensures reliable oxygen transport and simultaneously improves the power balance of the fuel cell. Both aspects are highly relevant for practical applications, where long-term durability and efficiency gains determine the competitiveness of fuel cell technology.

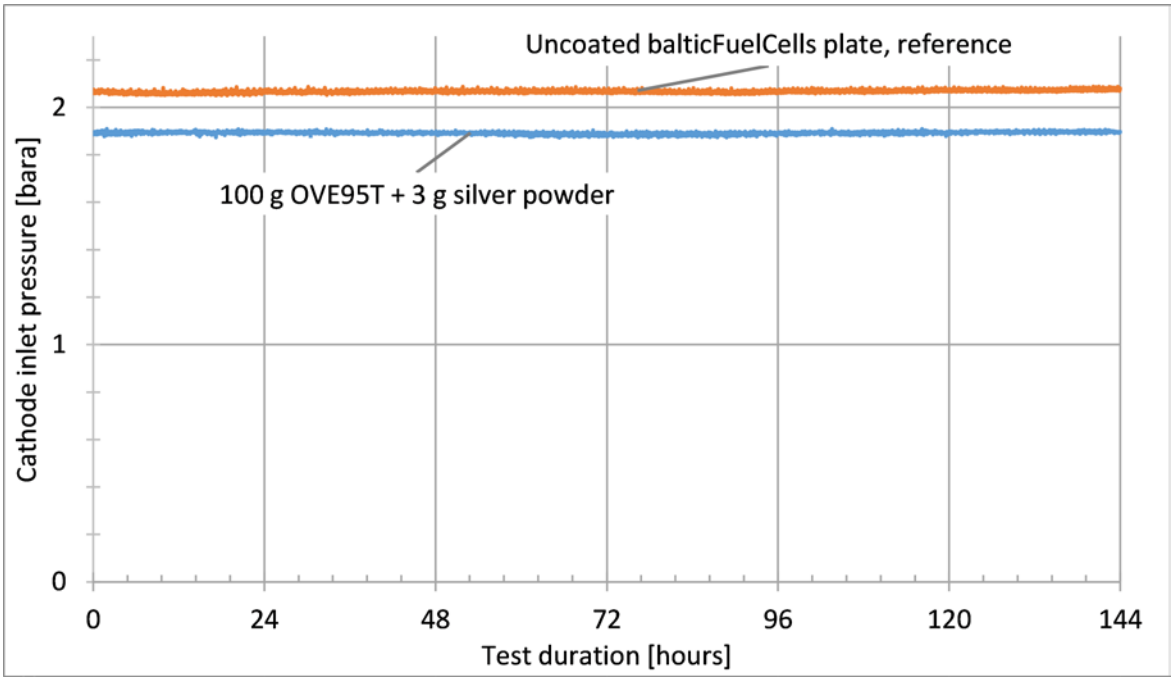

Figure 11. Cathode inlet pressure during long-term operation at T = 80 °C and 100 % relative humidity. The diagram shows the cathode-side pressure profiles over a test duration of 144 hours for the balticFuelCells plates. The coated plate exhibits a consistently lower cathode pressure compared to the reference plate, indicating reduced flow resistance in the coated system. Both curves remain stable throughout the entire measurement period.

5. Discussion

The investigated coatings were evaluated with respect to wettability, electrical conductivity, and fuel cell performance in single-cell tests. Among the tested systems, the OVE95T formulation with silver powder proved to be the most promising. Static contact angle measurements revealed strongly hydrophobic surfaces with angles well above 130°, which remained stable even at elevated temperatures. This indicates that the coating effectively reduces surface wettability and promotes the formation of compact droplets, a prerequisite for efficient water removal in the fuel cell flow field. Dynamic measurements further confirmed that droplets formed on the coated plates adopt a spherical shape, although contact angle hysteresis indicates some degree of pinning. In practice, however, the shear forces in operating cells assist droplet detachment, making the coating suitable for continuous operation.

Equally important, the incorporation of silver powder ensured that the coating remained electrically conductive. The measured resistances were only slightly higher than the uncoated reference, but still low enough to prevent significant ohmic losses. This demonstrates that the filler forms a conductive network within the binder matrix, enabling a balance between hydrophobicity and conductivity. Two properties that are typically difficult to combine in a single coating.

The single-cell polarization measurements showed that the coated and uncoated plates exhibit nearly identical performance across the entire current range. This finding highlights that the coating does not impair electrochemical activity or introduce additional resistive losses, but instead maintains performance at the level of the reference. Long-term operation at constant voltage further supported this conclusion. While the absolute current of the coated plate was slightly lower, the stability of the current output confirmed the coating’s robustness under continuous load.

In the conducted experiments, only the cathode-side bipolar plate was replaced with the coated variant, since the majority of the product water is generated and removed on this side of the cell. Consequently, the modification of a single plate has only a minor influence on the overall ohmic resistance of the system, which is dominated by other components such as the membrane, gas diffusion layers, and contact resistances within the cell assembly. This explains why no significant increase in ohmic resistance is apparent in the polarization curve, despite the higher intrinsic resistivity of the coated plate material. The coated plate, however, demonstrates improved water removal, as evidenced by a lower pressure drop on the cathode side during operation. This indicates a more efficient evacuation of liquid water from the flow field.

Moreover, this enhanced water management likely contributes to the improved cell performance, particularly in the concentration loss region of the polarization curve. By facilitating a more uniform distribution of reactants and reducing local flooding effects, the coating supports more stable gas transport and electrochemical activity across the electrode area. As a result, the coated plate not only maintains comparable ohmic behavior but can even lead to enhanced overall performance under conditions where mass transport limitations typically dominate.

A particularly advantageous effect was observed in the cathode pressure measurements. Cells with OVE95T coatings consistently operated at a lower cathode pressure compared to the reference. Since cathode compression consumes a significant fraction of system power, reducing this demand directly increases the net efficiency of the fuel cell. Thus, even though the short-term current density was somewhat reduced, the system-level benefit of lower auxiliary power consumption can translate into higher overall efficiency.

In summary, the OVE95T coating with silver powder offers a promising wet-coating solution for graphite bipolar plates. It combines high and thermally stable hydrophobicity with sufficient conductivity, maintains cell performance comparable to uncoated plates, and contributes to reduced parasitic power demand through lower cathode pressures. This makes it an innovative approach to improve water management and efficiency in PEM fuel cell systems.

6. References

[1] Irshad H and Shahgaldi S 2025 Comprehensive review of bipolar plates for proton exchange membrane fuel cells, *International Journal of Hydrogen Energy*, **111**, 462-487.

[2] Liu J, Zhang L, Yuan B, Zhang Y, Yang Z and Huang J 2024 Design and development of coating for metallic bipolar plates, *Materials & Design*, **246**, 113338.

[3] Ijaodola O, Ogungbemi E, Nisar F, Wilberforce T, Ramadan M, El Hassan Z, Thompson J and Olabi A 2018 Evaluating the Effect of Metal Bipolar Plate Coating on the Performance of Proton Exchange Membrane Fuel Cells, *Energies*, **11**(11), 3203.
[4] Shojaei S, Ehsan R and Frej M 2024 A review on key factors influencing the electrical properties of polymer-based bipolar plates, *Polymers for Advanced Technologies* **35**(2), e6301.
[5] U.S. Department of Energy 2025 DOE Technical Targets for Polymer Electrolyte Membrane Fuel Cell Components, https://www.energy.gov/.
[6] Ingle AV 2024 Corrosion and Its Mitigation Approaches of Metallic Bipolar Plates, *In book: Corrosion and Degradation in Fuel Cells, Supercapacitors and Batteries* (pp.33-69).
[7] Lee YB and Lim DS 2010 Electrical and corrosion properties of stainless steel bipolar plates, *Current Applied Physics*, **10** (2), S18-S21.
[8] Zhao X, Wang Z, Xiao LZY, Deng G, Li S, Cai Z and Liu S 2025 Corrosion-Resistant and Conductive Coatings on 316L Stainless Steel Bipolar Plates Fabricated by Hot Rolling, Materials, **18**(8) 1831.
[9] Bohackova T, Ludvik L and Kouril M 2021 Metallic Material Selection and Prospective Surface Modification for Bipolar Plates: A Review, *Materials*, **14**, 2682.
[10] Li W, Xie Z, Qiu S, Zeng H, Liu M and Wu G 2023 Improved Performance of Composite Bipolar Plates for PEM Fuel Cells with CNT Addition, *Nanomaterials*, **13**, 365.
[11] Antolini E and Passos R 2025 Si based and Si containing compounds in composite matrices and coatings for bipolar plates/interconnects, and in sealant materials for fuel cells, *Materials for Renewable and Sustainable Energy* **14,** 33.
[12] Niu Z, Wang X, Li Y, Huang F, He Z, Deng Q, Hu F and Zhou Q 2025 Review of Conductive Polymer Coatings for Metallic Bipolar Plates in Proton Exchange Membrane Fuel Cells, *Journal of Polymer Materials*, **42**(1).
[13] Narasimharaju S, Rau P and Annamalai K 2024 Advancement and characterization of Nitride Coating Materials on Aluminum Alloy-based Bipolar plates in PEMFC's Applications, MATEC Web of Conferences 393, 01010.
[14] OVE Plasmatec GmbH, [Online]. Available: https://www.ove-plasmatec.de.
[15] Kwok D and Neumann A, "Contact angle measurement and contact angle interpretation," Advances in Colloid and Interface Science, 81 (1999) 167-249, https://doi.org/10.1016/S0001-8686(98)00087-6.
[16] balticFuelCells quickCONNECTfixture, [Online]. Available: https://balticfuelcells.de/htmdocs/de/download/bFC_Flyer_qCf-LC-25_100.pdf. [Accessed 10 09 2025].
[17] HORIBA FuelCon [Online]. Available: https://www.horiba-fuelcon.com/core-testsysteme.
[18] DataPhysics Instruments GmbH, OCA product series DataPhysics Instruments GmbH. [Online]. Available: https://www.dataphysics-instruments.com/ resources/Downloads/ OCA_EN.pdf.